Project Report
2008 MVK 160 *Heat and Mass Transport*
May 08, 2008, Lund, Sweden

Review of temperature distribution in cathode of PEMFC

Munir Ahmed Khan
Department of Energy Sciences, Lund Institute of Technology,
P.O. Box 118, 22100, Lund, Sweden

ABSTRACT

In this review, the velocity and temperature distribution in the porous cathode of PEMFC was studied. The velocity distribution for the cathode was reproduced here and was found almost comparable except for the velocity magnitude which was higher in my case as the model was more simplified. Also, the effect of Stanton Number on temperature distribution of the solid phase and fluid phase was studied and it was found that at lower Stanton number, the solid and fluid phases had different temperature profiles but as the Stanton number is increased and at a value of $\mathrm{St} = 1.47 \times 10^3$, both the phases are almost at the same temperature.

1. INTRODUCTION

Fuel cells can be compared to the conventional engines with the basic difference that in fuel cells instead of bio-fuel, hydrogen is burnt to release energy according to the following reaction;

$$2H_2 + O_2 \rightarrow 2H_2O \qquad (1)$$

The basic operation of a fuel cell can be seen pictorially in Fig. 1.

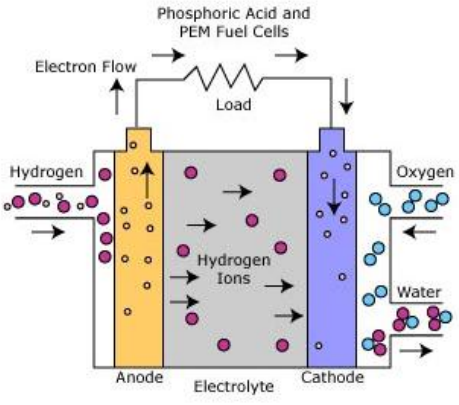

Fig. 1: PEMFC components and basic operation

Hydrogen (fuel) enters the anode side of the cell while oxygen enters on the cathode side. The hydrogen is oxidized at anode splitting it into electrons and protons.

$$2H_2 \rightarrow 4H^+ + 4e^- \qquad (2)$$

The cell is design as such that the products of the above reaction are made to travel through different paths i.e. electrons are forced to follow external path through a load and protons travel to the cathode side through an electrolyte (membrane) where they react with oxygen and electrons coming through external circuit to produce water.

$$O_2 + 4e^- + 4H^+ \rightarrow 2H_2O \qquad (3)$$

Clearly, for both the reactions at anode and cathode to proceed continuously, the cell must be supplied through a continuous source of both hydrogen and oxygen. And due to this, the fuel cells differ from batteries in that fuel cell can operate continuously as long as they are supplied with fuel.

The main feature of the fuel cells that made them a key research field in current era is there clean working, as the only product of the reactions in the fuel cells is water and high efficiency.

NOMENCLATURE

c_{H_2O}	Water vapor mole concentration
$c_{H_2O,ref}$	Normalized water vapor mole concentration at inlet

c_{O_2}	Oxygen concentration
$c_{O_2,ref}$	Oxygen mole concentration at inlet
c_p	Specific heat at constant temperature
$D_{O_2,eff}$	Effective diffusivity of oxygen in gas diffusion layer
k_C	Thermal conductivity of catalyst layer
p	Pressure
T	Temperature
u, v	Velocity components in x and y directions
St	Stanton number
Pt	Platinum

Greek symbols

α_1, α_2	Coefficients in Eq. (8)
δ	Thickness of diffusion layer
δ_C	Thickness of catalyst layer
ρ	density

2. MODELING APPROACHES FOR CATALYST LAYER

The catalyst layer has become a sensitive research domain of the fuel cells for current research activities. To date, three different modeling techniques have been applied to simulate the catalyst layer of PEMFC. The approaches are;

a) Thin film model
b) Discrete-volume model
c) Agglomerate model

Current research activities have mainly been focused on the agglomerate model as being the most comprehensive in describing the details of the catalyst layer that the other two models lacked in.

The discrete-volume approach resembles the agglomerate model except that the discrete-volume method doesn't incorporate the concept of agglomeration of catalyst particles. The thin film model being different of all is the least descriptive of any as it only considers the catalyst layer as a boundary condition between the membrane and porous transport layer (PTL) and neglects the physical thickness of the catalyst layer which is usually of order of microns.

3. CATALYST LAYER STRUCTURE

In agglomerate model, as described by Harvey et al. [4], the catalyst layer is considered to be compromised of agglomerates in which the Pt is dispersed on the carbon particles. The carbon particles are held in a polymeric electrolyte material.

A detailed study was performed on the structure of the catalyst layer by Siegel et al. [1]. In their work a piece of 5 cm^2 of MEA was studied under scanning electron microscope (SEM) and transmission electron microscope (TEM). Three different regimes of the catalyst structure can be indentified in Fig. 2 as Pt particles, carbon support and the ionomer. Fig. 2 explains the clumping phenomena of the Pt particles that can help in understanding the under utilization of the catalyst by reducing the surface area.

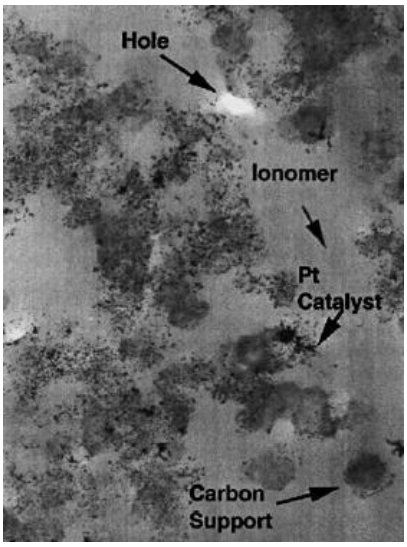

Fig. 2: TEM image of an agglomerate (18,400x).

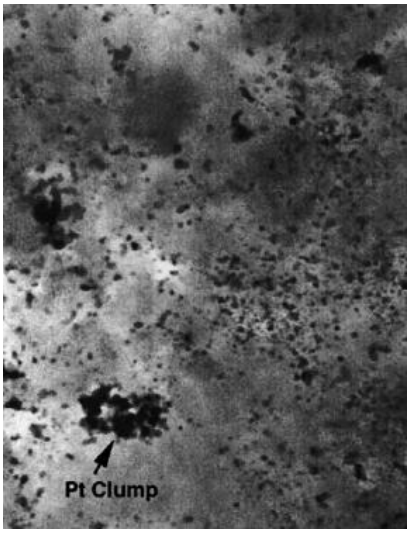

Fig. 3: TEM image of an agglomerate showing Pt catalyst particles and clumping (48,5500x)

4. MATHEMATICAL MODELING OF CATHODE

In both diffusion layer and catalyst layer, the steady volume-averaged continuity and momentum equations are given by

$$\frac{\partial}{\partial x}(\rho_f u) + \frac{\partial}{\partial y}(\rho_f v) = S_c \quad (4)$$

$$\rho_f u\frac{\partial u}{\partial x} + \rho_f v\frac{\partial u}{\partial y} = -\frac{\partial p}{\partial x} + \mu\left(\frac{\partial^2 u}{\partial x^2} + \frac{\partial^2 u}{\partial y^2}\right) + S_u \quad (5)$$

$$\rho_f u\frac{\partial v}{\partial x} + \rho_f v\frac{\partial v}{\partial y} = -\frac{\partial p}{\partial y} + \mu\left(\frac{\partial^2 v}{\partial x^2} + \frac{\partial^2 v}{\partial y^2}\right) + S_v \quad (6)$$

All of the electro-chemical reactions occur in the catalyst layer. The energy equation for the catalyst layer is given as;

$$(\rho c_p)_f u\frac{\partial T_f}{\partial x} + (\rho c_p)_f v\frac{\partial T_f}{\partial y} = k_{C,eff}\left(\frac{\partial^2 T_f}{\partial x^2} + \frac{\partial^2 T_f}{\partial y^2}\right) + S_c \quad (7)$$

The source term S_c in Eq. (7) represents the overpotential heating by the electro-chemical reactions and is calculated as;

$$S_c = \left(\alpha_1\left(\frac{c_{O_2}}{c_{O_2,ref}}\right) - \alpha_2\left(\frac{c_{H_2O}}{c_{H_2O,ref}}\right)^2\right)\cdot\eta \quad (8)$$

The Eq. (8) contains the concentration values of both O_2 and H_2O along with their reference values usually taken at inlet, so, the energy equation is coupled with the species equation for both the constituents. The species transport of the oxygen and water vapor in the catalyst layer is given by;

$$u\frac{\partial c_{O_2}}{\partial x} + v\frac{\partial c_{O_2}}{\partial y} = D_{O_2,eff}\left(\frac{\partial^2 c_{O_2}}{\partial x^2} + \frac{\partial^2 c_{O_2}}{\partial y^2}\right) + S_{O_2} \quad (9)$$

Similarly, for water vapors, Eq. (9) can be utilized by using H_2O concentration and its source term. Similarly for diffusion layer, Eq. (7) and (9) are equally valid except that there are no electro-chemical reactions taking place there, so, for diffusion layer no source term is employed.

To be used in numerical analysis, all the equations hav to be discretized by introducing dimensionless ratios and numbers. The procedure and technique for discretization can be found in [5].

5. RESULTS

For the present study, only the velocity profile was reproduced as per given conditions and parameters in [2]. The geometry analyzed is given Fig. 3 and geometric parameters for the geometry are given in Table. 1.

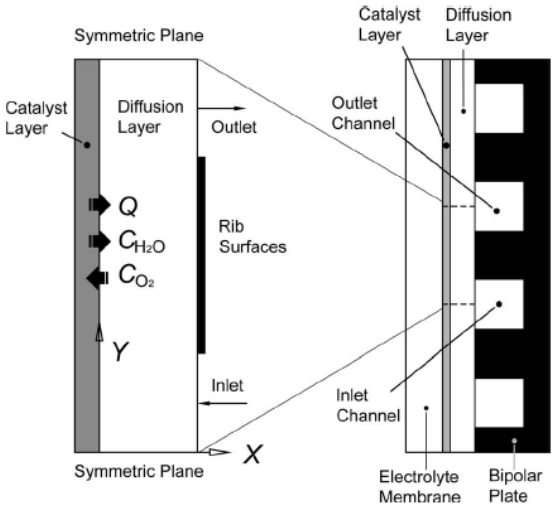

Fig. 4: Schematic drawing of porous electrode

Table 1: Geometric parameters for the analyzed domain

Geometric Parameters	Dimensions
Module Length	$L = 160\ \mu m$
Catalyst layer thickness	$\delta_c = 10\ \mu m$
Diffusion layer thickness	$\delta = 40\ \mu m$
Channel width	$2W = 80\ \mu m$
Shoulder Width	$Ws = 80\ \mu m$

The velocity profile obtained for the above configuration is in accordance with the results obtained by Chao [3] except for the velocity magnitude that was higher in this case as the approach was further simplified by the using the mixture model in which both oxygen and water vapor were considered to have the same velocities (Fig. 5).

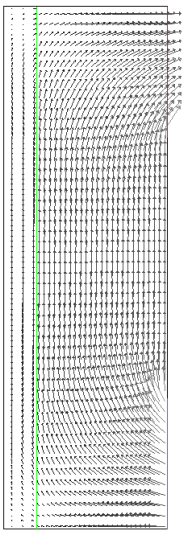

Fig. 5: Velocity distribution inside of porous cathode

It can be seen in Fig. 5 that velocity vectors have higher magnitude in the diffusion layer because of its higher porosity (0.48) and permeability ($1.57 \times 10^{-12}\ m^2$) as compared to the catalyst layer. Also the velocity magnitude

is higher in the shoulder area because of the shorter path and less pressure drop.

6. Discussion about Temperature Distribution in porous cathode

The results for the temperature distribution in porous cathode are presented in Fig. 5, 6 and 7 as simulated by Chao [3]. The comparison between the solid and fluid phases is made on the basis of Stantom number (Stantom number is defined in Appendix 'A')

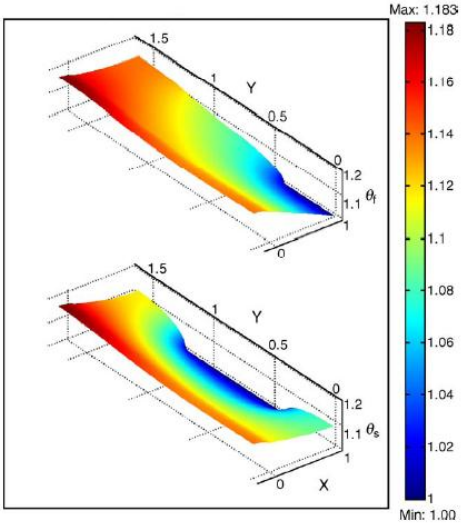

Fig. 6: Comparison of fluid phase and solid phase temperature distributions inside porous electrode, *St*=0.74

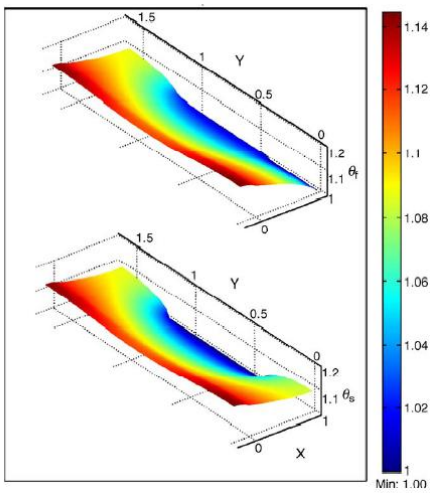

Fig. 7: Comparison of fluid phase and solid phase temperature distributions, *St*=14.73

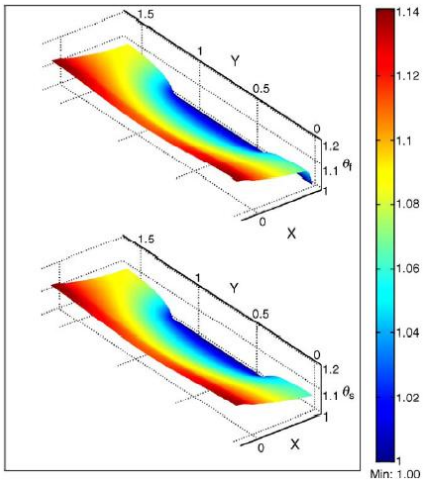

Fig. 8: Comparison of fluid phase and solid phase temperature distributions, $St = 1.47 \times 10^3$

The fluid phase temperature increases from inlet ($X = O$) of the module as the flow approaches the catalyst layer because of the electro-chemical reactions occurring in the catalyst layer. As can be seen in Fig. 5 that the solid phase temperature at the inlet is at higher level than the fluid phase. At the module inlet, the solid matrix transfers some heat to the incoming fluid via convection. But near the rib region, the fluid phase temperature is higher than the solid matrix indicating that the heat is not carried away by the bulk motion of the fluid only but is also convected into the solid and ultimately conducted away into the rib. But, as seen in Fig. 6, as the Stanton number is increased, the difference in the temperature of the two phases is decreased. It was observed that at $St = 1.47 \times 10^3$ the distribution of the fluid phase and solid phase temperatures are almost the same except at the module inlet.

The description of the Stanton number is given in Appendix 'A'.

APPENDIX 'A'

Stanton Number

In the present study, the Stanton number has been used as a reference parameter for the comparison of the solid and fluid phases temperature distributions because it characterizes heat transfer in forced convection flows. Stanton number for heat transfer, *St*, is a dimensionless parameter relating heat transfer coefficient to heat capacity of the fluid stream per unit cross-sectional area per unit time [6].

$$St = \frac{\alpha}{\dot{m} c_p} \qquad (10)$$

Also, as defined in [7], the stantom number can be calculated as

$$St = \frac{Nu}{Re\ Pr} = \frac{h}{c_p \rho V} \qquad (11)$$

REFERENCES

[1] Siegel, N. P., M. W. Ellis, D. J. Nelsen, M. R. von Spakovsky. "Single domain PEMFC model based on agglomerate catalyst geometry." Journal of Power Sources 115(2003): 81-89.

[2] Hwang, J. J.. "Heat transfer in porous electrode of fuel cells." Journal of Heat Transfer 128(2006): 434.

[3] Chao, C. H., Azai J. J. Hwang. "Prediction of phase temperature in a porous cathode of polymer electrolyte fuel cells using a two-equation model." Journal of Power Sources 160(2006): 1122-1130.

[4] Harvey, D., J. P. Pharoah, K. Karan. "A comparison of different approaches to modeling of PEMFC catalyst layer." Journal of Power Sources 179(2008): 209-219.

[5] Hwang, J. J., C.H. Chao, W. Y. Ho, C.L. Chang, D.Y. Wang. "Effect of flow orientation on thermal-electrochenical transports in a PEM fuel cell." Journal of Power Sources 157(2006): 85-97.

[6] "Stantom number."International Encyclopedia of Heat and Mass Transfer. "1st ed". 1996.

[7] "Stantom Number." Wikipedia. 8 May 2008 <http://en.wikipedia.org/wiki/Stanton_number>.